JACS
JOURNAL OF THE AMERICAN CHEMICAL SOCIETY
Article
pubs.acs.org/JACS

Multiple-Site Concerted Proton–Electron Transfer Reactions of Hydrogen-Bonded Phenols Are Nonadiabatic and Well Described by Semiclassical Marcus Theory

Joel N. Schrauben,[†,‡] Mauricio Cattaneo,[§,†] Thomas C. Day,[†] Adam L. Tenderholt,[†,∥] and James M. Mayer*[,†]

[†]Department of Chemistry, University of Washington, Seattle Washington 98195, United States

Supporting Information

ABSTRACT: Photo-oxidations of hydrogen-bonded phenols using excited-state polyarenes are described to derive fundamental understanding of multiple-site concerted proton–electron transfer reactions (MS-CPET). Experiments have examined phenol bases having $-CPh_2NH_2$, $-Py$, and $-CH_2Py$ groups *ortho* to the phenol hydroxyl group and *tert*-butyl groups in the 4,6-positions for stability (**HOAr-NH$_2$**, **HOAr-Py**, and **HOAr-CH$_2$Py**, respectively; Py = pyridyl; Ph = phenyl). The photo-oxidations proceed by intramolecular proton transfer from the phenol to the pendent base concerted with electron transfer to the excited polyarene. For comparison, 2,4,6-^{t}Bu$_3$C$_6$H$_2$OH, a phenol without a pendent base and *tert*-butyl groups in the 2,4,6-positions, has also been examined. Many of these bimolecular reactions are fast, with rate constants near the diffusion limit. Combining the photochemical k_{CPET} values with those from prior thermal stopped-flow kinetic studies gives data sets for the oxidations of **HOAr-NH$_2$** and **HOAr-CH$_2$Py** that span over 10^7 in k_{CPET} and nearly 0.9 eV in driving force ($\Delta G^{o\prime}$). Plots of log(k_{CPET}) vs $\Delta G^{o\prime}$, including both excited-state anthracenes and ground state aminium radical cations, define a single Marcus parabola in each case. These two data sets are thus well described by semiclassical Marcus theory, providing a strong validation of the use of this theory for MS-CPET. The parabolas give $\lambda_{CPET} \cong 1.15-1.2$ eV and $H_{ab} \cong 20-30$ cm^{-1}. These experiments represent the most direct measurements of H_{ab} for MS-CPET reactions to date. Although rate constants are available only up to the diffusion limit, the parabolas clearly peak well below the adiabatic limit of ca. 6×10^{12} s^{-1}. Thus, this is a very clear demonstration that the reactions are nonadiabatic. The nonadiabatic character slows the reactions by a factor of ~45. Results for the oxidation of **HOAr-Py**, in which the phenol and base are conjugated, and for oxidation of 2,4,6-^{t}Bu$_3$C$_6$H$_2$OH, which lacks a base, show that both have substantially lower λ and larger pre-exponential terms. The implications of these results for MS-CPET reactions are discussed.

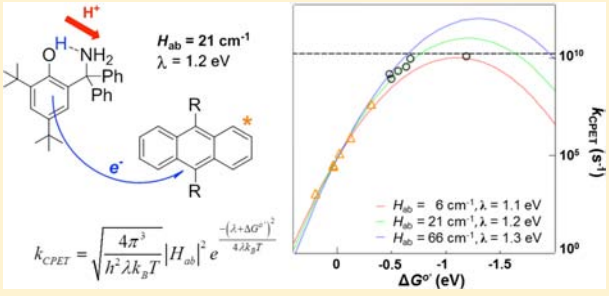

INTRODUCTION

Proton-coupled electron-transfer (PCET) reactions are integral to a wide range of processes, including oxygen production and reduction in photosynthesis, mitochondria and fuel cells, catalytic nitrogen fixation, and hydrocarbon oxidations. Because of this widespread importance, PCET has been studied in many contexts via experiments, computations, and new theoretical approaches.[1−4] Of most interest are reactions in which proton transfer (PT) and electron transfer (ET) occur in a single kinetic step, termed concerted proton–electron transfer (CPET) reactions. Despite the widespread attention on these reactions, questions remain about the conceptual and practical models that should be used. The key question addressed here is whether these reactions should be treated as adiabatic or nonadiabatic. Most chemical reactions are treated as adiabatic processes, occurring on a single free energy surface. Electron-transfer reactions, however, are typically considered to be nonadiabatic transitions from a reactant surface to a product surface. This nonadiabatic nature means that they have maximum reaction rates below ca. 6×10^{12} s^{-1} under barrierless conditions, as described below. Most of the theoretical treatments of CPET start from nonadiabatic models, as described in a recent special issue of *Chemical Reviews*.[1] The same issue of *Chemical Reviews* contains an extensive review of computational (typically DFT) studies of PCET reactions, which almost invariably assume adiabatic reactivity.[5] It has been proposed that the extent of nonadiabaticity in these processes is the most direct distinction between different types of reactions under the PCET umbrella.[6,7] This proposal comes mostly from theorists, because it is experimentally challenging to evaluate nonadiabatic character in a reaction.

To probe fundamental questions in PCET, we and others have used model systems incorporating phenols. These studies are also relevant to biological energy production, biosynthesis, and antioxidant activity.[8] Biological tyrosine oxidations involve

Received: June 11, 2012
Published: September 13, 2012

proton transfer (PT) and form the neutral tyrosyl radical. The most notable example is the oxidation of Y_Z in photosystem II that occurs with proton movement to a hydrogen-bonded histidine base (H-bonds to aspartate, glutamate, and lysine residues are also biologically relevant).[8−10] Linschitz and co-workers were the first to study phenol oxidations in which the proton transfers to a base concerted with ET to a separate oxidant,[11,12] which can be termed multiple-site concerted proton-electron transfer (MS-CPET). These studies have been extended in many ways, including thermal, photochemical, and electrochemical oxidations.[10−42] Our group[21−24,29] and others[19,20,25−27,41] have examined intramolecular H-bonded phenols as mimics of the Y_Z-His site in PSII,[10,25] and Hammarström, Meyer, Nocera, and others have tethered phenol or tyrosine derivatives to photo-oxidants.[10,18,19,31−40]

These phenol MS-CPET reactions have been analyzed with various levels of theory. A few papers have applied versions of Hammes-Schiffer's multistate continuum theory, although this is challenging, and simplifications usually have to be applied because many of the needed parameters are not easily accessible.[22,32,43−49] More typically, versions of the semiclassical Marcus theory of ET have been used (eq 1).[19,21−23,28,29,33,42,50−54] This has also been applied to electrochemical CPET, via the Marcus−Hush−Levich formalism.[15−17,20,27,41,55−57]

$$k_{\mathrm{CPET}} = \sqrt{\frac{4\pi^3}{h^2\lambda k_B T}}\,|H_{ab}|^2 e^{\frac{-(\lambda+\Delta G^{o'})^2}{4\lambda k_B T}} \quad (1)$$

Equation 1 gives the rate constant in terms of the corrected reaction driving force $\Delta G^{o'}$, the intrinsic barrier λ, an H_{ab} coupling parameter, the temperature T, and the Boltzmann and Planck constants. H_{ab} is the electronic coupling between the reactant and the product diabatic (noninteracting) states and is the quantitative measure of nonadiabaticity. At the crossing point of the diabatic states, this coupling causes a mixing of two diabatic states into two adiabatic states separated by $2H_{ab}$. When H_{ab} is more than k_BT (207 cm^{-1} at 25 °C), the system predominantly stays on the lower surface and can be treated as an adiabatic reaction, as occurring on a single surface.[58] As noted above, this is the typical situation for most chemical reactions. When the coupling is smaller, the reaction is nonadiabatic and there is only a small probability that the reactants will progress to products when they have the nuclear configuration of the crossing region.

Here we determine the extent of adiabaticity in MS-CPET reactions of H-bonded phenols by mapping the Marcus parabola of rate constant versus driving force. At the top of this parabola the free energy barrier is zero because the driving force is the same magnitude as the reorganization energy ($\Delta G^{o'} = -\lambda$). The rate constant at the top of the parabola is a direct measure of the nonadiabaticity and H_{ab}. This is the approach that Gray et al. have used to measure the distance dependence of H_{ab} and ET rate constants.[59,60] Adiabatic reactions have maximum first-order rate constants of ~6×10^{12} s^{-1} (k_BT/h, the Eyring prefactor).[58] Equation 1 gives a 6×10^{12} s^{-1} prefactor at T = 298 K with λ = 1.2 eV (as appropriate for the compounds here) when H_{ab} = 160 cm^{-1}. Conceptually, when the top of the parabola is close to $k = 6 \times 10^{12}$ s^{-1}, the reaction can be considered adiabatic, while lower peak rate constants indicate the importance of the nonadiabatic character. For instance, the reactions of excited-state Ru^{II}−diimine complexes with cytochrome c are significantly nonadiabatic, with H_{ab} ~ 1 cm^{-1} and ET parabolas that peak at $k = 3 \times 10^8$ s^{-1}.[61]

Reported here are rate constants for MS-CPET oxidation of H-bonded phenols from time-resolved fluorescence quenching experiments, employing excited-state polyarenes as photo-oxidants (Scheme 1). Combining these data with previously reported stopped-flow measurements from our laboratory[21,23,24,62] gives a set of rate constants from 10^3 M^{-1} s^{-1} to the diffusion limit of $10^{10.2}$ M^{-1} s^{-1}, with driving forces $\Delta G^{o'}$

Scheme 1. (A) Kinetic Scheme for Phenol-Base MS-CPET and (B) Phenols, Photo-Oxidants, and Oxidants

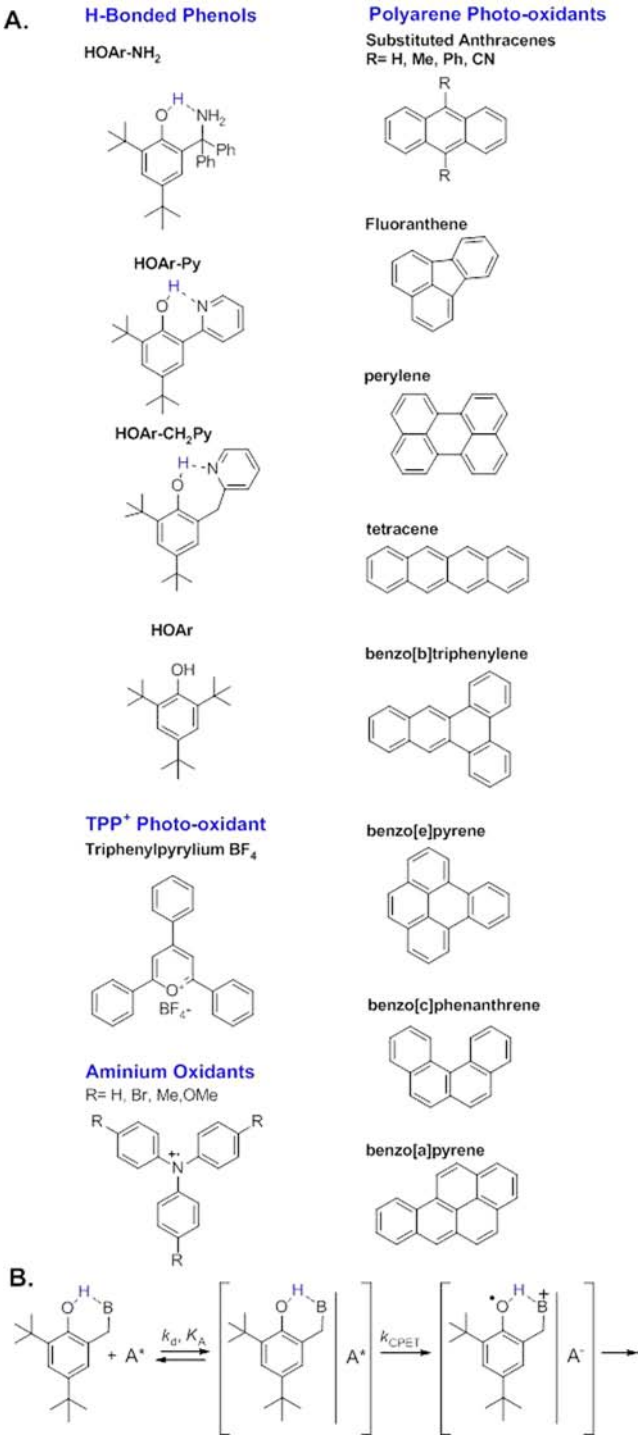

dx.doi.org/10.1021/ja305668h | J. Am. Chem. Soc. 2012, 134, 16635−16645

from +0.2 to nearly −2 eV. This data set describes a parabola truncated by the diffusion limit and is well-analyzed using the semiclassical Marcus model. These experiments provide the most direct measure to date of the nonadiabaticity of these biologically and technologically relevant transformations.

EXPERIMENTAL SECTION

General. Unless otherwise noted, all reagents were purchased from Aldrich. Acetonitrile (HPLC grade) was purchased from EMD (results were identical when 'low water brand' acetonitrile from Burdick and Jackson was used). Deuterated solvents were purchased from Cambridge Isotope Laboratories. **HOAr-NH$_2$**,[24] **HOAr-Py**,[63] and **HOAr-CH$_2$Py**[21] were prepared by literature methods, and 2,4,6-tri*tert*-butylphenol (2,4,6-^{t}Bu$_3$C$_6$H$_2$OH) was purchased from Aldrich and recrystallized from ethanol.

Physical Measurements. ^{1}H NMR spectra were recorded at ambient temperatures on Bruker AF300, AV300, AV301, DRX499, or AV500 spectrometers. UV−vis spectra were collected on an Hewlett-Packard 8453 diode array spectrophotometer. Steady-state fluorescence spectra were collected on a Perkin-Elmer LS-50B instrument.

Time-Correlated Single Photon Counting (TCSPC) was carried out using a PicoQuant FluoTime 100 time-resolved fluorescence spectrometer with the PicoHarp 300 stand-alone photon counting module in the Photonics Center at the University of Washington. Picosecond pulsed diode lasers (wavelengths: 375, 405, and 470 nm), controlled by the PDL 800-D driver, produce excitation pulses as short as 70 ps (fwhm) at a repetition rate of 80 MHz. A series of filters was employed to block the scatter of the excitation source. The acquisition counts per second was held at a value of ∼10^5 s^{-1}, much less than the fluorescence lifetime of the fluorophores (∼10^8 s^{-1} for most of the fluorophores used herein) to avoid instrumental artifacts. In general, the acquisition time was 5−10 min. A typical 2 mL sample consisted of 10 μM of the fluorophore in acetonitrile with 1−3% MeOH or MeOD. Bimolecular kinetics were measured by adding in a known amount of the phenol base of interest (the quencher), measuring the kinetics, and adding an additional three or four aliquots of the phenol in order to construct a Stern−Volmer plot [see Figure 1 and Supporting Information (SI)]. The quencher was typically added in 50−100 μL aliquots such that the final quencher concentration after three or four additions was 2−10 mM. Larger final concentrations of quencher were necessary for slower reactions with small fluorescence lifetimes. Three Stern−Volmer quenching rates were measured for each fluorophore/quencher combination to gauge the error of the measurement. Fits of the time-resolved fluorescence data to monoexponential decays were carried out using the FluoFit software package,[64] in which the instrument response function (IRF, obtained by scattering the excitation source into the detector using a water/Ludox suspension) was convoluted with an exponential decay to fit the data.

Examples of time-resolved fluorescence data sets and Stern−Volmer plots for this system can be found in Figure 1. Kinetic isotope effects were measured by adding an excess of MeOD (typically ∼1−3% of the total volume) to the acetonitrile solutions and measuring the fluorescence lifetime as a function of added quencher as described above. As a control, MeOH was added to measure k_H, with rate constants being within the uncertainty of measurements in pure acetonitrile.

Calculations. All DFT calculations were carried out in Gaussian 09[65] on the Stuart Cluster at the chemistry department at the University of Washington. Calculations were done at the UB3LYP/6-311++G(d,p) level with an acetonitrile PCM model. The self-exchange innersphere reorganization energy for the polyarenes, λ_i, was calculated according to the four-point model of Nelsen.[66,67] The value of λ_i for $[N(tol)_3]^{\bullet+}$ was taken to be characteristic for all $[N(Ar)_3]^{\bullet+}$, and thus no other four-point calculations were carried out for these oxidants. All ground-state calculations were shown to have no imaginary frequencies (using the freq = noraman keyword), except for that of 9-methylanthracene which displayed an imaginary methyl rotational mode. As a comparison, several time-dependent calculations of excited-state energies were carried out as described in the SI.

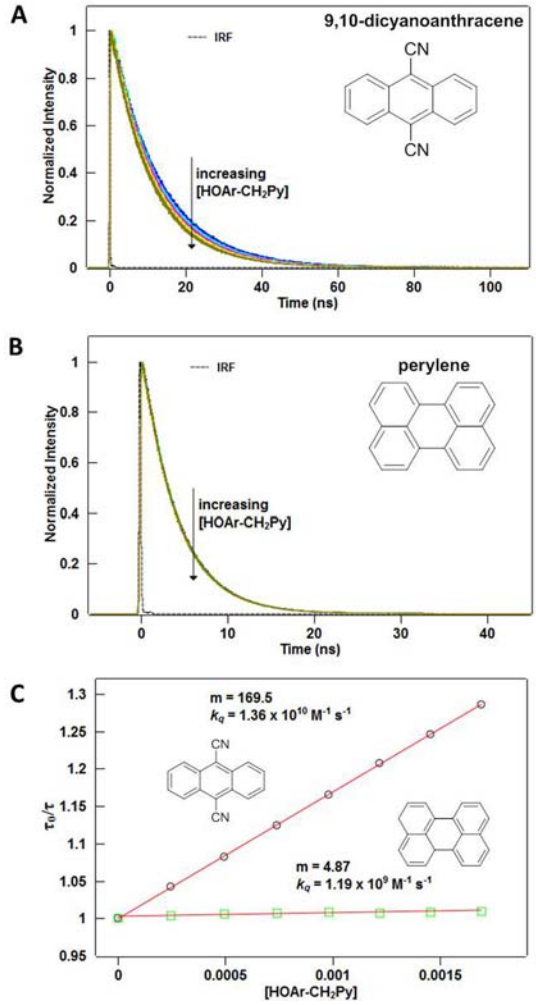

Figure 1. Examples of **HOAr-CH$_2$Py** quenching the fluorescence of (A) 9,10-dicyanoanthracene and (B) perylene. The IRF, which indicates the temporal width of the excitation pulse, is shown in both cases. (C) Stern−Volmer plots for these reactions, which allow calculation of the quenching rate constant (k_q) from the slope (m).

RESULTS AND DISCUSSION

Rate Constants and Driving Forces. The oxidations of phenols by excited-state polyarenes were monitored by time-resolved fluorescence quenching. Addition of increasing amounts of the phenol-base compounds decreases the lifetime of the fluorophore (Figure 1). In general, reactions proceeding with k_{obs} > 10^8 M^{-1} s^{-1} provided well-behaved monoexponential fluorescence decays. The changes in lifetime vary linearly with phenol concentration, giving quenching rate constants (k_{obs}) by standard Stern−Volmer analysis (Figure 1C, Table 1, and see SI). Correlation values for the Stern−Volmer plots were generally near R^2 = 1, although slower reactions did suffer a larger relative error.

Fluorescence quenching must involve ET rather than resonant energy transfer because the phenols are not significantly absorbing at the emission wavelengths of the fluorophores. The correlation of rate constants with excited-state reduction potential of the fluorophores (Table 1 and Figure 2) also points to quenching by ET. However, simple ET without proton movement is ruled out by its much less favorable driving force.[21,23,68] As shown in Table 1, rate constants of >10^9 M^{-1} s^{-1} have been measured for reactions

dx.doi.org/10.1021/ja305668h | J. Am. Chem. Soc. 2012, 134, 16635−16645

Table 1. Reaction driving force, observed quenching rate, and various corrections for three different H-bonded phenols with both polyarene photo-oxidants and aminium oxidants

	ΔG^{o}_{CPET} (eV)[a]	w (eV)[b]	$\Delta G^{o}_{CPET}{}'$ (eV)[c]	k_{obs} (M^{-1} s^{-1})[d]	k_{CPET} (s^{-1})[e]
			HOAr-NH$_2$		
[TPP](BF$_4$)[g]	−1.76	0.00	−1.76	1.3 ± 0.2 × 10^{10}	≥k_d[f]
9,10-dicyanoanthracene	−1.15	−0.03	−1.18	1.1 ± 0.1 × 10^{10}	≥k_d[f]
9-cyanoanthracene	−0.63	−0.04	−0.67	5.4 ± 1.0 × 10^{9}	8.3 × 10^{9}
anthracene	−0.59	−0.04	−0.63	2.7 ± 0.2 × 10^{9}	3.2 × 10^{9}
fluoranthene	−0.55	−0.04	−0.59	9.8 ± 1.0 × 10^{8}	1.1 × 10^{9}
9-phenylanthracene	−0.52	−0.03	−0.55	1.8 ± 0.1 × 10^{9}	2.0 × 10^{9}
benzo[b]triphenylene	−0.47	−0.04	−0.51	9.8 ± 5.0 × 10^{8}	1.0 × 10^{9}
9,10-diphenylanthracene	−0.46	−0.03	−0.49	7.6 ± 1.8 × 10^{8}	8.0 × 10^{8}
9-methylanthracene	−0.44	−0.04	−0.48	1.3 ± 0.2 × 10^{9}	1.4 × 10^{9}
perylene	−0.39	−0.04	−0.43	1.1 ± 0.1 × 10^{9}	1.2 × 10^{9}
benzo[c]phenanthrene	−0.36	−0.04	−0.40	2.0 ± 0.9 × 10^{8}	2.0 × 10^{8}
tetracene	−0.29	−0.03	−0.32	8.0 ± 1.1 × 10^{8}	8.4 × 10^{8}
benzo[a]pyrene	−0.21	−0.03	−0.24	6.2 ± 1.5 × 10^{8}	6.4 × 10^{8}
[N(*p*-C$_6$H$_4$Br)$_3$]$^{\bullet+}$	−0.31	0.00	−0.31	4 ± 2 × 10^{7}[j]	4 × 10^{7}
[N(*p*-C$_6$H$_4$OMe)(*p*-C$_6$H$_4$Br)$_2$]$^{\bullet+}$	−0.12	0.00	−0.12	8 ± 1 × 10^{5}[j]	8 × 10^{5}
[N(tol)$_3$]$^{\bullet+}$[h]	−0.02	0.00	−0.02	1.1 ± 0.2 × 10^{5}[j]	1.2 × 10^{5}
[N(*p*-C$_6$H$_4$OMe)$_2$(*p*-C$_6$H$_4$Br)]$^{\bullet+}$	0.04	0.00	0.04	2.7 ± 0.3 × 10^{4}[j]	2.7 × 10^{4}
[MPT]$^{\bullet+}$[i]	0.04	0.00	0.04	3.2 ± 0.3 × 10^{4}[j]	3.2 × 10^{4}
			HOAr-Py		
[TPP](BF$_4$)[g]	−1.55	0.00	−1.55	1.5 ± 0.2 × 10^{10}	≥k_d[f]
9,10-dicyanoanthracene	−0.94	−0.03	−0.97	1.4 ± 0.1 × 10^{10}	≥k_d[f]
9-cyanoanthracene	−0.42	−0.04	−0.46	9.1 ± 1.1 × 10^{9}	≥k_d[f]
anthracene	−0.38	−0.04	−0.42	1.2 ± 0.2 × 10^{10}	≥k_d[f]
fluoranthene	−0.34	−0.04	−0.38	5.4 ± 0.16 × 10^{9}	8.2 × 10^{9}
9-phenylanthracene	−0.31	−0.03	−0.34	1.1 ± 0.09 × 10^{10}	≥k_d[f]
9,10-diphenylanthracene	−0.25	−0.03	−0.28	7.4 ± 0.79 × 10^{9}	≥k_d[f]
9-methylanthracene	−0.22	−0.04	−0.26	1.1 ± 0.05 × 10^{10}	≥k_d[f]
perylene	−0.18	−0.04	−0.22	7.4 ± 0.49 × 10^{9}	≥k_d[f]
benzo[c]phenanthrene	−0.15	−0.04	−0.19	6.0 ± 0.10 × 10^{9}	9.6 × 10^{9}
tetracene	−0.08	−0.03	−0.11	3.9 ± 0.49 × 10^{9}	5.2 × 10^{9}
benzo[a]pyrene	0.00	−0.03	−0.03	6.0 ± 0.95 × 10^{9}	9.7 × 10^{9}
			HOAr-CH$_2$Py		
[TPP](BF$_4$)[g]	−1.69	0.00	−1.69	1.4 ± 0.2 × 10^{10}	≥k_d[f]
9,10-dicyanoanthracene	−1.08	−0.03	−1.11	1.1 ± 0.2 × 10^{10}	≥k_d[f]
9-cyanoanthracene	−0.56	−0.04	−0.60	6.7 ± 1.3 × 10^{9}	1.2 × 10^{10}
anthracene	−0.52	−0.04	−0.56	4.4 ± 0.4 × 10^{9}	6.0 × 10^{9}
fluoranthene	−0.48	−0.04	−0.52	1.0 ± 0.1 × 10^{9}	1.1 × 10^{9}
9-phenylanthracene	−0.45	−0.03	−0.48	1.4 ± 0.2 × 10^{9}	1.5 × 10^{9}
benzo[e]pyrene	−0.42	−0.03	−0.45	1.2 ± 0.1 × 10^{9}	1.3 × 10^{9}
9,10-diphenylanthracene	−0.39	−0.03	−0.42	1.3 ± 0.4 × 10^{9}	1.4 × 10^{9}
9-methylanthracene	−0.37	−0.04	−0.41	7.5 ± 0.4 × 10^{8}	7.9 × 10^{8}
perylene	−0.32	−0.04	−0.36	5.8 ± 1.8 × 10^{8}	6.1 × 10^{8}
benzo[c]phenanthrene	−0.29	−0.04	−0.33	6.3 ± 1.5 × 10^{8}	6.6 × 10^{8}
benzo[a]pyrene	−0.14	−0.03	−0.17	5.5 ± 2.5 × 10^{8}	5.7 × 10^{8}
[N(*p*-C$_6$H$_4$OMe)(*p*-C$_6$H$_4$Br)$_2$]$^{\bullet+}$	−0.04	0.00	−0.04	5.3 ± 0.5 × 10^{5}[k]	5.3 × 10^{5}
[N(tol)$_3$]$^{\bullet+}$[h]	0.06	0.00	0.06	1.2 ± 0.1 × 10^{5}[k]	1.2 × 10^{5}
[N(*p*-C$_6$H$_4$OMe)$_3$]$^{\bullet+}$	0.28	0.00	0.28	8 ± 2 × 10^{2}[k]	8 × 10^{2}
	ΔG^{o}_{ET} (eV)[l]	w (eV)[b]	$\Delta G^{o}_{ET}{}'$ (eV)[c]	k_{obs} (M^{-1} s^{-1})[d]	k_{CPET} (s^{-1})[e]
			2,4,6-^{t}Bu$_3$C$_6$H$_2$OH		
[TPP](BF$_4$)[g]	−0.95	−0.03	−0.98	1.5 ± 0.1 × 10^{10}	≥k_d[f]
9,10-dicyanoanthracene	−0.34	−0.03	−0.37	8.6 ± 1.5 × 10^{9}	≥k_d[f]
9-cyanoanthracene	0.18	−0.04	0.14	2.4 ± 0.5 × 10^{9}	2.8 × 10^{9}
anthracene	0.22	−0.04	0.18	~6 × 10^{7}[m]	~6 × 10^{7}

[a]Calculated by the Rehm−Weller equation, eq 3, for photo-oxidations, using $E(D^+/D)_{CPET}$. These potentials therefore correspond to those of the CPET process. [b]From eq 4, using the equivalent radii of Tables S4 and S5. [c]From eq 4.[75] [d]Average and 1 standard deviation from three measurements with ~1−5% MeOH added by volume. [e]Calculated using eq 2, taking k_D = $10^{10.2}$ M^{-1} s^{-1} and K_A = 1 M^{-1}; error bars are similar to those for k_{obs} except are larger when k_{obs} approaches k_d. [f]Because k_{obs} is very close to the diffusion limit, $10^{10.2}$ M^{-1} s^{-1}, the data only show that $k_{H,CPET} \geq k_d$. [g]2,4,6-triphenylpyrylium tetrafluoroborate. [h]Tri-*p*-tolylaminium. [i]10-Methylphenothiazinium. [j]Values reported in ref 23. [k]Values reported in ref 21. [l]Calculated using eq 3 with $E(D^+/D)_{ET}$, which is 0.6−0.8 eV more positive than $E(D^+/D)_{CPET}$ for photo-oxidation involving the

dx.doi.org/10.1021/ja305668h | J. Am. Chem. Soc. 2012, 134, 16635−16645

Table 1. continued

same polyarene. [m]Measuring this slow rate required extremely high phenol concentrations which could affect the characteristic radiative dynamics of the fluorophore, so the uncertainty on this value is larger than the ~2% estimated error from fitting the fluorescence data.

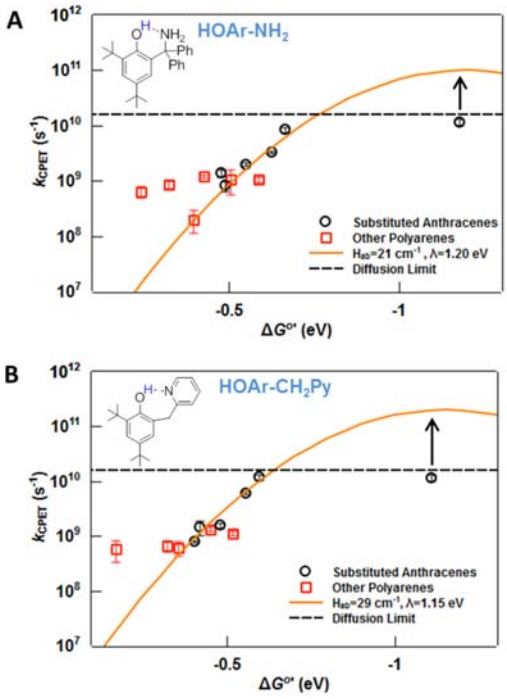

Figure 2. Plots of photochemical k_{CPET} values vs $\Delta G^{o\prime}$ for (A) **HOAr-NH$_2$** and (B) **HOArCH$_2$Py**. The points for the reaction with TPP^+ (the most exergonic of the photo-oxidations) occur at the diffusion limit and have been removed to allow for an expanded *x*-axis. The remaining points at the diffusion limit are indicated as lower limits. A curve that represents a good fit of eq 1 to the substituted anthracene data (black circles) is provided in each case.

with CPET driving forces of −0.43 eV (**HOAr-NH$_2$**), −0.03 eV (**HOAr-Py**), and −0.42 eV (**HOAr-CH$_2$Py**). Such high rate constants would not be possible for ET processes that are 0.60−0.80 eV less favorable.

The importance of PT is also indicated by the substantially larger rate constants for the **HOAr-B** quenchers vs 2,4,6-^{t}Bu$_3$C$_6$H$_2$OH, which cannot undergo proton loss, with the same photo-oxidant. For example, with anthracene as the photo-oxidant, $k > 10^9$ M^{-1} s^{-1} for all three **HOAr-B** but $k \cong 6 \times 10^7$ M^{-1} s^{-1} for the same reaction with 2,4,6-^{t}Bu$_3$C$_6$H$_2$OH, in the absence of an appended base. In a few cases, we observe kinetic isotope effects (KIEs) $k_H/k_D > 1.5$ (although the uncertainties in these measurements are high, see SI), which is also an indication of a CPET reaction. KIEs close to unity are still consistent with CPET, as has been discussed theoretically and seen experimentally.[69] Finally, we note that mechanisms of initial pre-equilibrium PT followed by ET (termed PTET) were ruled out in earlier studies with these phenols, based on the very unfavorable initial PT step.[23]

Thus in essentially all of the cases, the fluorescence quenching is due to ET from the phenol base to the fluorophore concerted with intramolecular PT from the phenol to the base. As noted above, such a MS-CPET mechanism has been shown to be followed by the phenols used here reacting with weaker oxidants,[21,23,24,62] and as shown below, there is good correspondence between the thermal and photoinduced rate constants. In general, oxidations of such H-bonded phenols have been shown to be CPET reactions,[8−12,16−23,27,29,33,56,62,70,71] although Hammarström and co-workers have found exceptions.[18,19]

For reactions near the diffusion limit, diffusion and CPET are kinetically coupled to give the observed rate, k_{obs}. Following the standard Marcus treatment of ET, diffusion forms a precursor complex with rate constant k_d and equilibrium constant K_A, and k_{CPET} is taken as the first-order rate constant for CPET within this complex (Scheme 1A). For each of the phenols in this study at least several reactions occurred at the diffusion limit, as evidenced by a plateauing of k_{obs} for the most exergonic reactions, and k_d was determined empirically to be $10^{10.2}$ M^{-1} s^{-1} from an average of these values. When k_{obs} is close to k_d, k_{CPET} is calculated according to eq 2, with the standard assumption that $K_A \cong 1$ M^{-1}.[72] Uncertainties in the calculated values of k_{CPET} that stem from the chosen values of K_A and k_d are discussed below.

$$\frac{1}{k_{obs}} = \frac{1}{k_d} + \frac{1}{k_{CPET}K_A} \quad (2)$$

The driving force for photoinduced ET rate constants such as these is typically calculated by the method of Rehm and Weller (eq 3). This approach has been questioned by a recent re-examination of the original Rehm−Weller data set. Farid et al. showed that the oxidations of substituted aryl compounds by excited-state polyarenes can involve a significant role for fluorescent exciplexes, so that the typical Marcus formalism cannot be applied.[73,74] For the reactions studied here, steady-state fluorescence spectra indicate no fluorescing exciplexes across the entire span of driving forces, indicating that the Rehm−Weller equation is appropriate for calculating ΔG^o for these reactions. However, in some instances of 'slow' quenching, i.e., $\Delta G^o > -0.1$ eV and $k_{obs} < 10^8$ M^{-1} s^{-1}, the quenching observed by time-resolved fluorescence was not observed by steady-state fluorescence, and in some instances, steady-state measurements showed an increase in fluorescence quantum yield in the presence of the phenol base. This phenomenon can be accounted for by the large concentrations of phenol base affecting the radiative and nonradiative deactivation pathways, leading to an increased fluorescence quantum yield.[73] Thus these results do not represent true ET quenching of the polyarene fluorescence and are not included in this report. Otherwise, the driving force can be calculated by eq 3, and the data reported here can be analyzed by the Stern−Volmer approach.

The Rehm−Weller equation (eq 3) gives the driving force for photoinduced ET processes using the ground-state reduction potentials (E) and excited-state energies (ΔG_{00}). In this case, the measured reduction potential of the donor, $E(D^+/D)$, is for the CPET reaction, which includes the PT.[21,23] E and ΔG_{00} values for all compounds are given in the SI.

$$\Delta G^o = E(D^+/D)_{CPET} - E(A/A^-) - \Delta G_{00} \quad (3)$$

$$\Delta G^{o\prime} = \Delta G^o + w; \quad w = (Z_A - Z_D - 1)\frac{e^2}{Dr_{D^+A^-}} \quad (4)$$

The ET step in this reaction converts a precursor complex to a successor complex, D|A → $D^+|A^-$. In this case, the successor

dx.doi.org/10.1021/ja305668h | J. Am. Chem. Soc. 2012, 134, 16635−16645

complex is stabilized by the attraction of the opposite charges, and ΔG^{o} must be corrected for this energy. The stabilization is $-e^2/Dr_{D+|A-}$ (eq 4) for an excited neutral donor oxidizing a phenol, in which D is the static dielectric constant and $r_{D+|A-}$ is taken as the sum of the radii of the donor and acceptor. This term was calculated to be about −30 to −40 meV for all neutral donor/acceptor combinations here. This correction is not needed for reactions of cationic acceptors with neutral donors, such as the photochemical reactions of the triphenylpyrylium cation and the stopped-flow reactions using triarylaminium radical cations. In this situation, the ET step is $D|A^+ \rightarrow D^+|A$ which occurs with very little change in the electrostatic interaction so $w \cong 0$.

Analysis of the Rate Constants with the Semiclassical Marcus Equation. The rate constants measured here for photo-oxidation of **HOAr-NH$_2$** and **HOAr-CH$_2$Py** are plotted as a function of $\Delta G^{o\prime}$ in Figure 2. The estimated error bars are shown and are typically the size of the symbols or smaller. The rate constants for the reactions of substituted anthracenes are plotted with black circles, while the data for all of the other polyarenes are red squares. The rate constants for the substituted anthracenes follow the expected dependence of k_{CPET} on $\Delta G^{o\prime}$. To highlight this dependence, Figure 2 includes parabolic fits that are derived from the combined data sets in Figure 3, as described below.

The rate constants for the other polyarenes have a much flatter and more irregular dependence on $\Delta G^{o\prime}$. In the analyses below, we restrict our fitting to the data from the anthracene reactions, which follows most studies of photoinduced ET reactions in which a series of structurally similar oxidants is typically used.[11,12,73,74,76,77]

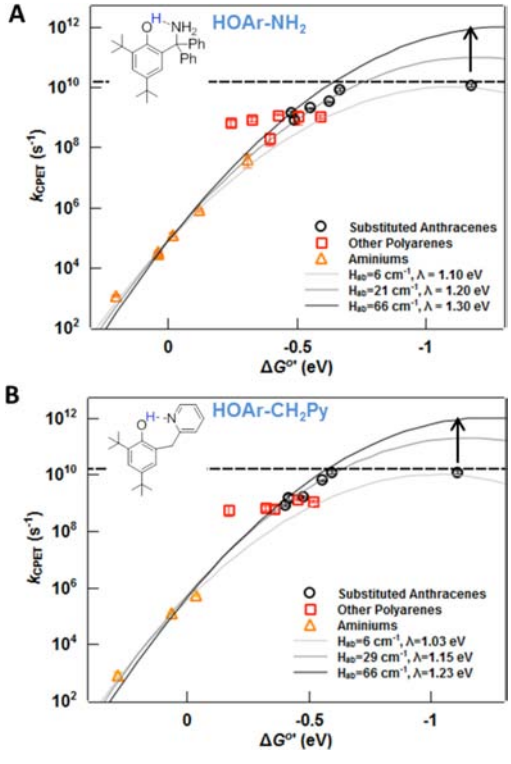

Figure 3. k_{CPET} plotted as a function of $\Delta G^{o\prime}$ for (A) **HOAr-NH$_2$** and (B) **HOAr-CH$_2$Py** for oxidation by both excited-state polyarenes (black circles and red squares) and aminiums (orange triangles). Note the log scale on the y-axis. Various Marcus parabolas with variable λ have been provided with pre-exponential terms spanning 10^{10}–10^{12} s^{-1}. The arrows in the plots indicate that these points, which were observed at the diffusion limit, are lower limits for k_{CPET}. The other polyarenes (red squares) are not considered in making the fits.

The irregular dependence of rate constants for polyarenes other than the anthracenes indicates that there are differences between these photo-oxidants other than their excited-state reduction potentials. Given their structural diversity, it is not surprising that reorganization energies and/or H_{ab} values vary over this series. Consistent with this, the farthest outliers from the parabolic fits below are generally the larger polyarenes, for both the **HOAr-NH$_2$** and the **HOAr-CH$_2$Py** reactions. To explore the origin of these irregularities, we have carried out independent calculations of the outer- and inner-sphere reorganization energies λ_o and λ_i. These are described in detail in the SI; only the approach and conclusions are summarized here. The λ_o and λ_i components are broken down into contributions from both the donor (the phenol) and the acceptor (excited-state arene). The λ_o values for both the phenols and polyarenes were estimated from an empirical relation using equivalent hard-shell radii,[55,78,79] and λ_i for the polyarenes was calculated using Nelsen's four-point model.[66,67] A formalism was developed for adjusting $\Delta G^{o\prime}$ for differences in the calculated λ, which took into account the best fit parameters for the substituted anthracene curve for each phenol base (see SI). The calculated values of λ for reactions involving the same phenol base, which included both the phenol and photo-oxidant contributions, generally differed by no more than 0.1 eV. The $\Delta G^{o\prime}$ data sets adjusted for these differences in λ still show significant outliers from the best fit. Thus differences in λ alone cannot account for the variation in k_{CPET}.

This analysis indicates that the reaction pairs that are outliers have different adiabaticities (different values of H_{ab}) from that of the best fit. The extent of the difference in adiabaticity was explored by maintaining the best-fit value of λ and optimizing H_{ab} for the adjusted data set to fit the Marcus parabola through the outlier points. This exercise indicated a substantially increased H_{ab} term, relative to that for the substituted anthracenes, for these outlier points. It is less likely that these outliers are a result of different values of K_A and k_d for the larger polyarenes (vide infra and SI).

Figure 3 plots the photochemical rate constants together with the previously determined thermal rate constants for oxidations of **HOAr-NH$_2$** and **HOAr-CH$_2$Py** with aminium ions from stopped-flow experiments (triangles).[21,22,62] The inverted parabolas in the figures are the predicted log(k) vs $\Delta G^{o\prime}$ curves from the semiclassical Marcus equation (eq 1), with the given values of H_{ab} and the reorganization energy λ. The stopped-flow rate constants and the anthracene photochemical rate constants as a function of driving force are described with good accuracy by the same Marcus parabola. In fact, the best-fit parameters shown in Figure 2 are retained with the expanded data set of Figure 3. The oxidations with aminium radical cations lie generally in the linear regime of the ET curve; therefore, many different ET curves that represent large spans in H_{ab} and λ can fit these data. That a single ET curve can be employed to model the entire data set is therefore not conclusive that the two sets of reactions share the same ET parameters. However, based on the mild curvature of the points for the aminium oxidations, the span of pre-exponential factors for eq 1 ("A") can be narrowed to $10^{10} < A < 10^{12}$ s^{-1} for **HOAr-NH$_2$** and $10^{8} < A < 10^{11}$ s^{-1} for **HOAr-CH$_2$Py**, indicating similar H_{ab} and λ values for both types of oxidations.

dx.doi.org/10.1021/ja305668h | J. Am. Chem. Soc. 2012, 134, 16635–16645

This is consistent with reported values of λ for tri-*p*-tolylamine$^{+/0}$ (0.51 eV in MeCN) and non-ion-paired anthracene$^{0/-}$ or tetracene$^{0/-}$ (both 0.38 eV in DMF).[75] The apparent equivalence of the reorganization energies and H_{ab} values for the anthracene photooxidations and the aminium thermal oxidations is reasonable given the similar size of these oxidants (both with three aromatic rings) and their somewhat localized charge (at the nitrogen in $NAr_3^{\bullet+}$ and on the central ring in anthracene$^{\bullet-}$).

The combined stopped-flow and photochemical data sets are very well fit by the semiclassical Marcus equation (eq 1), over 10^7 in k_{CPET}. This is a strong validation of the use of this equation to analyze CPET rate constants. Many years ago, Marcus predicted that this approach would hold for proton and atom transfers in this driving force regime, where $-\Delta G^{o} < \lambda$.[80−82] The semiclassical Marcus equation is much simpler than current theories of CPET, particularly in the treatment of the pre-exponential factor. In Hammes-Schiffer's multistate continuum theory, this pre-exponential term is a sum of Boltzmann-weighted Franck-Condon overlaps of vibronic states integrated over a range of proton donor-acceptor distances. This detailed analysis is conceptually very important and is needed to understand detailed issues such as H/D kinetic isotope effects. However, at least for these two compounds, the rate constants over a span of nearly 0.9 eV in $\Delta G^{o}_{CPET}{}'$ can be fit to good accuracy with a single H_{ab} overlap parameter and a single intrinsic barrier λ. It is not evident from the more complete and complex theories that H_{ab} should be essentially unchanged over such a range of reaction energies, especially given the importance of vibrational excited states in many cases.

The three parabolas drawn in Figure 3 have pre-exponential factors that span from 10^{10}−10^{12} s^{-1}. For both phenol bases, only ET curves with $A \cong 10^{11}$ s^{-1} are successful in modeling the entire data set. For reactions of **HOAr-NH$_2$**, the parabola is defined by λ = 1.2 eV and $A = 10^{11}$ s^{-1}, which implies H_{ab} = 21 cm^{-1}. For **HOAr-CH$_2$Py**, the derived values are similar: λ = 1.15 eV, $A = 10^{11.3}$ s^{-1}, and H_{ab} = 29 cm^{-1}. If the conservative estimate of ±20−30 meV is made for the uncertainty of each variable in eqs 3 and 4, then the uncertainty in the corrected driving force $\Delta G^{o\prime}$ is 30−40 meV, about the size of the points in Figures 2 and 3. Therefore, the Marcus parabolas in Figures 2 and 3 that fall on the points represent accurate estimates of the Marcus parameters; placing the fit outside of these points gives significantly different values of λ and/or H_{ab}.

The situation is markedly different for the **HOAr-Py** system (Table 1, Figure S1). All of the photochemical rate constants k_{obs} are $\geq 4 \times 10^9$ M^{-1} s^{-1}, even at driving forces as low as $\Delta G^{o\prime}$ = −0.03 eV. The k_{CPET} values for reactions with substituted anthracenes are all $\geq k_d$. No thermal rate constants are available with aminium ions, because the reactions even at $\Delta G^{o}_{CPET}{}' = 0$ are too fast to measure with stopped-flow mixing.[21,23] Therefore a detailed analysis similar to those above is not possible, and H_{ab} or λ cannot be determined. Still, these data are consistent with the conclusion based on stopped-flow measurements with iron-tris(diimine) oxidants that at $\Delta G^{o}_{CPET}{}' \cong 0$, **HOAr-Py** reacts roughly 2 orders of magnitude faster than **HOAr-NH$_2$** and **HOAr-CH$_2$Py**.[21,23] The k_{obs} for the 9-phenylanthracene photo-oxidation of **HOAr-Py** reported here is almost at the diffusion limit, $1.1 \pm 0.1 \times 10^{10}$ M^{-1} s^{-1} at $\Delta G^{o\prime}$ = −0.34 eV, while the values for the analogous oxidations of **HOAr-NH$_2$** and **HOAr-CH$_2$Py** are almost an order of magnitude slower despite having larger driving forces: $1.8 \pm 0.1 \times 10^9$ M^{-1} s^{-1} at $\Delta G^{o\prime}$ = −0.55 eV and $1.4 \pm 0.2 \times 10^9$ M^{-1} s^{-1} at $\Delta G^{o\prime}$ = −0.48 eV, respectively. Consistent with these results, our computational estimate of λ for the reaction of **HOAr-Py** + excited anthracene (see SI) is ∼0.2 eV less than the corresponding values for either **HOAr-NH$_2$** or **HOAr-CH$_2$Py**.

2,4,6-^{t}Bu$_3$C$_6$H$_2$OH is 0.6−0.8 V more difficult to oxidize than the phenols with pendent bases.[8,23] These reactions likely proceed by rate-limiting ET followed by PT to the solvent or to the reduced arene. The 0.6−0.8 V difference in potential is the energetic benefit of transferring the proton concerted with ET, the advantage of CPET over ET for the phenol-base compounds. The high potential for the oxidation of 2,4,6-^{t}Bu$_3$C$_6$H$_2$OH limits the number of photochemical polyarene reactions that can be studied by the TCSPC method to only the most oxidizing photo-oxidants. Still, when ET from 2,4,6-^{t}Bu$_3$C$_6$H$_2$OH has the same driving force as CPET from the phenol bases, 2,4,6-^{t}Bu$_3$C$_6$H$_2$OH is more reactive. For instance, 2,4,6-^{t}Bu$_3$C$_6$H$_2$OH transfers an electron to the 9-cyanoanthracene excited state at $2.8 \pm 0.5 \times 10^9$ M^{-1} s^{-1} despite the reaction being 0.14 eV uphill (Figure S1). This is consistent with prior studies showing that CPET is usually energetically favored over ET but is intrinsically more difficult.[18,23,24,33,36] Note that the high rates of oxidation of 2,4,6-^{t}Bu$_3$C$_6$H$_2$OH are achieved only with much stronger oxidants than used for the phenol-base compounds, because the ET reduction potential for 2,4,6-^{t}Bu$_3$C$_6$H$_2$OH is much higher than the PCET reduction potential for **HOAr-B**. The data available for 2,4,6-^{t}Bu$_3$C$_6$H$_2$OH do not indicate directly whether the slower rate constants for CPET vs ET at the same driving force are due to CPET having a higher intrinsic barrier λ or being more nonadiabatic (lower H_{ab}), although indirect assessments are possible, vide infra.

Uncertainties in the values of H_{ab} for the **HOAr-NH$_2$** and **HOAr-CH$_2$Py** data sets stem in part from uncertainties in the values of K_A and k_d, which affect k_{CPET} via eq 2. We have used the typical value of K_A = 1 M^{-1}; Sutin has argued that K_A should have a value less than 1, while following Eberson an estimate of 2 M^{-1} is obtained.[58,83,84] A change in K_A by a factor f would change H_{ab} by $f^{-1/2}$, e.g., a 40% increase in H_{ab} if K_A is taken as 0.5 M^{-1}. The value of k_d ($10^{10.2}$ M^{-1} s^{-1}) was determined from the many measured rates near this value. If this value is in error or is different for the different reagents, this would significantly affect k_{CPET} for reactions with k_{obs} near the diffusion limit. However, the value of k_d does not affect k_{CPET} when k_{obs} is more than an order of magnitude smaller than k_d. Choosing a value smaller than the apparent k_d, such as 10^{10} s^{-1}, changes the best-fit values only slightly because of the curvature of points with $k_{obs} \leq 10^9$ M^{-1} s^{-1} (Figure S2).

λ and H_{ab} Values: Nonadiabaticity of the Phenol Oxidations. The dependence of the rate constants on $\Delta G^{o\prime}$ (Figure 3) shows that CPET oxidations of **HOAr-NH$_2$** and **HOAr-CH$_2$Py** by aminium ions or excited polyarenes are mildly nonadiabatic. The H_{ab} values of 20−30 cm^{-1} are well below the 207 cm^{-1} (k_BT) value for adiabatic processes. Stated another way, the pre-exponential factors from the fits above, $\log(A)$ = 11−11.3 for **HOAr-NH$_2$** and **HOAr-CH$_2$Py**, are significantly lower than the Eyring prefactor k_BT/h in TS theory, $\log(6 \times 10^{12}\ s^{-1})$ = 12.8 at 298 K. These reactions, however, are not as nonadiabatic as ET between many transition metal systems, where H_{ab} can be 1 cm^{-1} or less.[61,85] Thus the nonadiabatic character of the **HOAr-NH$_2$** and **HOAr-CH$_2$Py** reactions reduces their rate constants by factors of ca. 60 and 30, respectively, versus what would be

dx.doi.org/10.1021/ja305668h | J. Am. Chem. Soc. 2012, 134, 16635−16645

predicted for an adiabatic reaction. In simple terms, the developers of CPET theories are correct that nonadiabatic effects are both conceptually and quantitatively important. On the other hand, this slowing of the rate constant by a factor of ~45 is within the uncertainty of *ab initio* or DFT calculations for solution reactions of this complexity[86] (a decrease by a factor of 40 in k results from an increase in $\Delta G^{\ddagger}$ of 2.2 kcal mol^{-1}). Thus it is reasonable for computational chemists to neglect nonadiabatic effects when calculating rate constants and energy surfaces for PCET reactions of this kind.

Several reports discuss the extent of nonadiabaticity in this family of reactions. These studies used various assumptions to simplify eq 1 to allow extraction of λ and/or H_{ab}. Our laboratory used a variable temperature stopped-flow study, of oxidations of **HOAr-NH$_2$** by aminiums and **HOAr-Py** by tris-diimine ferric complexes, to indicate lower limits for H_{ab} of ca. 10 and 6 cm^{-1}.[23] Costentin et al. re-evaluated these data using new electrochemical results and a different version of eq 1, finding λ = 0.8 eV for **HOAr-NH$_2$** and that the reactions are nonadiabatic with a transmission coefficient on the order of 0.005 (H_{ab} ~ 14 cm^{-1}).[27] For the closely related aminophenol HOAr-CH$_2$NC$_4$H$_8$, these researchers estimated λ = 0.7 eV based on electrochemical measurements,[20] then later reported λ = 1.06 eV for this aminophenol and that this electrochemical reaction is adiabatic.[27,41] A later analysis that took into account the distance dependence of the reaction revealed λ = 1.4 eV for HOAr-CH$_2$NC$_4$H$_8$ and λ = 1.5 eV for **HOAr-NH$_2$** and mild nonadiabaticity for these reactions.[87,88] Their analysis also indicated that excited proton vibrational states play a small role in the reaction. In contrast, Thorp and Meyer's study of intermolecularly H-bonded tyrosines with Ru or Os photo-oxidants found that k_{CPET} varied monotonically with ΔG^{o}_{CPET} and that a single-mode model was insufficient to explain the data, therefore concluding that vibronic levels above υ = 0 participate in the CPET process.[49] The H_{ab} term has been explored by Hammarström and co-workers for similar photo-oxidations by Ru complexes. A Ru-tyrosine conjugate was concluded to have H_{ab} = 5 cm^{-1} and λ = 1.2 eV for pure ET versus H_{ab} = 7 cm^{-1} and λ = 2.4 eV for the related CPET reaction (as determined via variable pH and temperature data; this large value of λ was determined without taking the increase in proton entropy with temperature into account).[33] In a different report the oxidation of a phenol-carboxylate intramolecular species by excited Ru(bpy)$_3^{2+}$ was explored; λ = 0.9–1.2 eV was determined, and no value for H_{ab} was given.[19] Overall, it appears that the nonelectrochemical determinations of λ and H_{ab} for **HOAr-NH$_2$** and similar systems roughly agree with the values determined in this report, with the exception of the value of λ determined in reference.[27] In all cases, save the earlier reports of electrochemical oxidations of aminophenols, these reactions were concluded to be mildly nonadiabatic.

The method used in this paper presents the most direct method for measuring λ and H_{ab}, i.e., by monitoring the rate of the reaction as a function of driving force and fitting the data to eq 1. The collection of data close to the top of the Marcus parabola, as presented herein, is essential to accurate elucidation of these parameters. Future studies in our laboratory will extend these studies to unimolecular reactions that are not limited by diffusion and will therefore be able to probe closer to the top of the parabola.

Theoretical studies suggest that the degree of electron–proton nonadiabaticity is related to the extent of charge distribution in a PCET process, with large redistribution of charge corresponding to a nonadiabatic process.[1,6,89,90] This predicts that the limiting examples of hydrogen atom transfer (HAT), in which the e^- and the H^+ transfer together from a single location to another, will be an adiabatic process. In contrast, MS-CPET processes should be nonadiabatic, with maximum rate constants slower than those for HAT.[1,89,91] The results reported here provide support for the latter prediction. The former prediction is also supported by previous work from our lab on HAT reactions. For a large set of HAT reactions, the classical (adiabatic) version of Marcus theory holds well in most cases.[28,50,51,54]

The intrinsic barriers of 1.20 and 1.15 eV for **HOAr-NH$_2$** and **HOAr-CH$_2$Py** are larger than typical λ values for simple organic ET reactions. For instance, ET self-exchange of the aminium ions used in the stopped-flow measurements has λ = 0.5 eV (assuming an adiabatic reaction).[75] Similarly, the data suggest that ET from 2,4,6-^{t}Bu$_3$C$_6$H$_2$OH is intrinsically easier than CPET of **HOAr-NH$_2$** and **HOAr-CH$_2$Py**. The outer-sphere (solvent) reorganization energies are likely not so different for ET and CPET for these molecules, as the proton moves only a short distance (~0.7 Å) within the phenol base.[22] The higher values of λ for **HOAr-NH$_2$** and **HOAr-CH$_2$Py** are therefore likely due to higher inner-sphere reorganization energies, particularly distortions that reduce the proton donor–acceptor distance and thereby facilitate CPET.[22,43] Still, the λ values of slightly more than 1 eV are in a range that is reasonable for biological reactions, consistent with the involvement of tyrosine-base ET cofactors.[10,60,92]

The CPET reactions of **HOAr-NH$_2$** and **HOAr-CH$_2$Py** are very similar in their λ and H_{ab} parameters, while the reactions of **HOAr-Py** are much more facile. The total reorganization energy for the reactions of **HOAr-Py**, **HOAr-NH$_2$**, and **HOAr-CH$_2$Py** with anthracene can be calculated using Nelsen's four-point model[66] for λ_i contributions and an empirical method for calculating the λ_o contributions.[21,62,93] These calculations indicate that λ for the reaction of **HOAr-Py** and anthracene is ~0.2 eV smaller than the calculated values for the reactions of the unconjugated phenol bases. The much faster reactions of **HOAr-Py**, despite the fact that pyridine is a weaker base than the primary amine, were ascribed to conjugation of the pyridine with the phenol and the resulting resonance-assisted H-bond.[21] For the reaction of **HOAr-Py** with excited substituted anthracenes, the k_{CPET} rate constants, being at least 10^{10} s^{-1}, and the calculated value of $\lambda_{CPET} \cong 1$ eV imply that $A \geq 10^{12}$ s^{-1} and $H_{ab} \geq 60$ cm^{-1}. These values provide the Marcus parabola with the smallest pre-exponential factor that can account for all of the reactions of the substituted anthracenes having $k_{CPET} \geq k_d$. These calculations and estimates indicate that the more facile reactions of **HOAr-Py** stem from not only a smaller inner-sphere reorganization energy but also from greater coupling.

The Marcus equation (eq 1) famously predicts an inverted region for ET, where the rate constants decrease with more negative driving forces ($-\Delta G^{o\prime} > \lambda$). In systems examined here, the reactions of the excited-state triphenylpyrylium cation are predicted to be in the inverted region (Figure 2 and Table 1), but they all occur at the diffusion limit. No evidence of inverted behavior is seen. Even for ET, the lack of inverted region is a general result for bimolecular reactions[75,85] (with a few exceptions, cf., refs 61, 85, 94, and 95). This has been attributed to charge transfer occurring at increasing distances in solution as the driving force is increased, which changes the reorganization energy.[75] Recent theoretical work concluded

that the inverted region is very likely inaccessible for CPET (unless the PT distance increases with driving force).[82] In addition, the triphenylpyrylium ion excited state is so oxidizing that the observed quenching could occur by simple ET, without proton movement, and still occur at the diffusion limit. While the lack of observation of an inverted region for CPET is not surprising, this is one of the rare experimental tests in that region.

CONCLUSIONS

A central question in fundamental studies of MS-CPET is whether these reactions should be considered adiabatic or nonadiabatic. In this study of H-bonded phenol-base compounds, the oxidations by photoexcited anthracenes and by aminium radical cations are shown to be nonadiabatic by direct experimental measurements. The rate constants for two different phenols, over a range of $>10^7$ in k_{CPET} and almost 0.9 eV in driving force ($\Delta G^{o\prime}$), are well described by semiclassical Marcus theory. For **HOAr-NH$_2$** and **HOArCH$_2$Py**, each set of data is well fit by a single Marcus parabola, with $\lambda_{CPET} \cong 1.15-1.20$ eV and $H_{ab} \cong 20-30$ cm^{-1}. It is significant that for each of the phenols, the whole data set can be fit with a single intrinsic barrier and vibronic coupling parameter H_{ab}. For the phenol-pyridine compound **HOAr-Py**, the fast rate constants appear to be due to both a smaller reorganization energy and a larger H_{ab}, both likely resulting from the conjugation between the phenol and the base. For all three phenol bases, the H_{ab} values are indicated to vary significantly for structurally different polyarene photo-oxidants.

The nonadiabatic character of the reactions reduces their rate constants by about a factor of ca. 45 versus an adiabatic reaction with the same free-energy barrier. Thus CPET theories that emphasize the importance of nonadiabaticity are correct that this is a significant effect for the experimentally measured kinetics of these reactions. On the other hand, computational studies are not introducing substantial error by ignoring nonadiabaticity because the factor of ~45 in rate constant is within the uncertainty of the calculations for such complex solution-phase reactions. That semiclassical Marcus theory can model the rates of these reactions over 7 orders of magnitude implies that complicated theoretical approaches are not necessarily required in the modeling of rate constants for this family of reactions.

ASSOCIATED CONTENT

Supporting Information

Materials and methods, additional figures, and a calculations of reorganization energies. This material is available free of charge via the Internet at http://pubs.acs.org.

AUTHOR INFORMATION

Corresponding Author

mayer@chem.washington.edu

Present Addresses

[‡]National Renewable Energy Laboratory, 15013 Denver West Parkway, Golden, CO 80401

[§]INQUINOA-CONICET, Instituto de Química Física, Facultad de Bioquímica, Química y Farmacia, Universidad Nacional de Tucumán, Ayacucho 471, (T4000INI) San Miguel de Tucumán, Argentina

[∥]Target Discovery, Inc., Palo Alto, CA 94303

Notes

The authors declare no competing financial interest.

ACKNOWLEDGMENTS

We are grateful for financial support from the U.S. National Institutes of Health (GM-50422 and an ARRA collaborative supplement to that award). The UW Chemistry computing facilities have been generously supported by the University of Washington Student Technology Fee Program.

REFERENCES

(1) Hammes-Schiffer, S.; Stuchebrukhov, A. A. *Chem. Rev.* **2010**, *110*, 6939.
(2) Cukier, R. I. *Biochim. Biophys. Acta, Bioenerg.* **2004**, *1655*, 37.
(3) Cukier, R. I.; Nocera, D. G. *Annu. Rev. Phys. Chem.* **1998**, *49*, 337.
(4) Iyengar, S. S.; Sumner, I.; Jakowski, J. *J. Phys. Chem. B.* **2008**, *112*, 7601.
(5) Siegbahn, P. E. M.; Blomberg, M. R. A. *Chem. Rev.* **2010**, *110*, 7040.
(6) Hammes-Schiffer, S. *J. Phys. Chem. Lett.* **2011**, *2*, 1410.
(7) Hammes-Schiffer, S. *Energy Environ. Sci.* **2012**, *5*, 7696.
(8) Warren, J. J.; Tronic, T. A.; Mayer, J. M. *Chem. Rev.* **2010**, *110*, 6961.
(9) Meyer, T. J.; Huynh, M. H. V.; Thorp, H. H. *Angew. Chem., Int. Ed.* **2007**, *46*, 5284.
(10) Dempsey, J. L.; Winkler, J. R.; Gray, H. B. *Chem. Rev.* **2010**, *110*, 7024.
(11) Biczók, L.; Gupta, N.; Linschitz, H. *J. Am. Chem. Soc.* **1997**, *119*, 12601.
(12) Biczók, L.; Linschitz, H. *J. Phys. Chem.* **1995**, *99*, 1843.
(13) Shukla, D.; Young, R. H.; Farid, S. *J. Phys. Chem. A* **2004**, *108*, 10386.
(14) Concepcion, J. J.; Brennaman, M. K.; Deyton, J. R.; Lebedeva, N. V.; Forbes, M. D. E.; Papanikolas, J. M.; Meyer, T. J. *J. Am. Chem. Soc.* **2007**, *129*, 6968.
(15) Bonin, J.; Costentin, C.; Louault, C.; Robert, M.; Savéant, J.-M. *J. Am. Chem. Soc.* **2011**, *133*, 6668.
(16) Bonin, J.; Costentin, C.; Robert, M.; Saveant, J.-M. *Org. Biomol. Chem.* **2011**, *9*, 4064.
(17) Bonin, J.; Costentin, C.; Robert, M.; Savéant, J.-M.; Tard, C. *Acc. Chem. Res.* **2012**, *45*, 372.
(18) Sjodin, M.; Ghanem, R.; Polivka, T.; Pan, J.; Styring, S.; Sun, L.; Sundstrom, V.; Hammarstrom, L. *Phys. Chem. Chem. Phys.* **2004**, *6*, 4851.
(19) Sjödin, M.; Irebo, T.; Utas, J. E.; Lind, J.; Merényi, G.; Åkermark, B.; Hammarström, L. *J. Am. Chem. Soc.* **2006**, *128*, 13076.
(20) Costentin, C.; Robert, M.; Savéant, J.-M. *J. Am. Chem. Soc.* **2006**, *128*, 4552.
(21) Markle, T. F.; Mayer, J. M. *Angew. Chem., Int. Ed.* **2008**, *47*, 738.
(22) Markle, T. F.; Rhile, I. J.; Mayer, J. M. *J. Am. Chem. Soc.* **2011**, *133*, 17341.
(23) Rhile, I. J.; Markle, T. F.; Nagao, H.; DiPasquale, A. G.; Lam, O. P.; Lockwood, M. A.; Rotter, K.; Mayer, J. M. *J. Am. Chem. Soc.* **2006**, *128*, 6075.
(24) Rhile, I. J.; Mayer, J. M. *J. Am. Chem. Soc.* **2004**, *126*, 12718.
(25) Maki, T.; Araki, Y.; Ishida, Y.; Onomura, O.; Matsumura, Y. *J. Am. Chem. Soc.* **2001**, *123*, 3371.
(26) Benisvy, L.; Blake, A. J.; Collison, D.; Stephen Davies, E.; David Garner, C.; McInnes, E. J. L.; McMaster, J.; Whittaker, G.; Wilson, C. *Dalton T.* **2003**, 258.
(27) Costentin, C.; Robert, M.; Savéant, J.-M. *J. Am. Chem. Soc.* **2007**, *129*, 9953.
(28) Mayer, J. M. *Acc. Chem. Res.* **2011**, *44*, 36.
(29) Markle, T. F.; Rhile, I. J.; DiPasquale, A. G.; Mayer, J. M. *Proc. Natl. Acad. Sci. U.S.A.* **2008**, *105*, 8185.
(30) Bronner, C.; Wenger, O. S. *J. Phys. Chem. Lett.* **2011**, *3*, 70.
(31) Johannissen, L. O.; Irebo, T.; Sjödin, M.; Johansson, O.; Hammarström, L. *J. Phys. Chem. B* **2009**, *113*, 16214.

(32) Zhang, M. T.; Irebo, T.; Johansson, O.; Hammarstrom, L. *J. Am. Chem. Soc.* **2011**, *133*, 13224.
(33) Sjödin, M.; Styring, S.; Wolpher, H.; Xu, Y.; Sun, L.; Hammarström, L. *J. Am. Chem. Soc.* **2005**, *127*, 3855.
(34) Reece, S. Y.; Nocera, D. G. *J. Am. Chem. Soc.* **2005**, *127*, 9448.
(35) Magnuson, A.; Berglund, H.; Korall, P.; Hammarstrom, L.; Akermark, B.; Styring, S.; Sun, L. C. *J. Am. Chem. Soc.* **1997**, *119*, 10720.
(36) Sjodin, M.; Styring, S.; Akermark, B.; Sun, L. C.; Hammarstrom, L. *J. Am. Chem. Soc.* **2000**, *122*, 3932.
(37) Westlake, B. C.; Brennaman, M. K.; Concepcion, J. J.; Paul, J. J.; Bettis, S. E.; Hampton, S. D.; Miller, S. A.; Lebedeva, N. V.; Forbes, M. D. E.; Moran, A. M.; Meyer, T. J.; Papanikolas, J. M. *Proc. Natl. Acad. Sci. U.S.A.* **2011**, *108*, 8554.
(38) Irebo, T.; Reece, S. Y.; Sjodin, M.; Nocera, D. G.; Hammarstrom, L. *J. Am. Chem. Soc.* **2007**, *129*, 15462.
(39) Lachaud, F.; Quaranta, A.; Pellegrin, Y.; Dorlet, P.; Charlot, M.-F.; Un, S.; Leibl, W.; Aukauloo, A. *Angew. Chem., Int. Ed.* **2005**, *44*, 1536.
(40) Moore, G. F.; Hambourger, M.; Gervaldo, M.; Poluektov, O. G.; Rajh, T.; Gust, D.; Moore, T. A.; Moore, A. L. *J. Am. Chem. Soc.* **2008**, *130*, 10466.
(41) Costentin, C.; Robert, M.; Savéant, J.-M.; Tard, C. *Angew. Chem., Int. Ed.* **2010**, *49*, 3803.
(42) Osako, T.; Ohkubo, K.; Taki, M.; Tachi, Y.; Fukuzumi, S.; Itoh, S. *J. Am. Chem. Soc.* **2003**, *125*, 11027.
(43) Markle, T. F.; Tenderholt, A. L.; Mayer, J. M. *J. Phys. Chem. B* **2012**, *116*, 571.
(44) Carra, C.; Iordanova, N.; Hammes-Schiffer, S. *J. Phys. Chem. B* **2002**, *106*, 8415.
(45) Hatcher, E.; Soudackov, A. V.; Hammes-Schiffer, S. *J. Am. Chem. Soc.* **2004**, *126*, 5763.
(46) Iordanova, N.; Decornez, H.; Hammes-Schiffer, S. *J. Am. Chem. Soc.* **2001**, *123*, 3723.
(47) Ishikita, H.; Soudackov, A. V.; Hammes-Schiffer, S. *J. Am. Chem. Soc.* **2007**, *129*, 11146.
(48) Soudackov, A. V.; Hazra, A.; Hammes-Schiffer, S. *J. Chem. Phys.* **2011**, 135.
(49) Fecenko, C. J.; Thorp, H. H.; Meyer, T. J. *J. Am. Chem. Soc.* **2007**, *129*, 15098.
(50) Mayer, J. M. *J. Phys. Chem. Lett.* **2011**, *2*, 1481.
(51) Warren, J. J.; Mayer, J. M. *Proc. Natl. Acad. Sci. U.S.A.* **2010**, *107*, 5282.
(52) Zieba, A. A.; Richardson, C.; Lucero, C.; Dieng, S. D.; Gindt, Y. M.; Schelvis, J. P. M. *J. Am. Chem. Soc.* **2011**, *133*, 7824.
(53) Yoder, J. C.; Roth, J. P.; Gussenhoven, E. M.; Larsen, A. S.; Mayer, J. M. *J. Am. Chem. Soc.* **2003**, *125*, 2629.
(54) Mayer, J. M. *Annu. Rev. Phys. Chem.* **2004**, *55*, 363.
(55) Saveant, J.-M. *Elements of Molecular and Biomolecular Electrochemistry: An Electrochemical Approach to Electron Transfer Chemistry*; John Wiley & Sons, Inc.: Hoboken, NJ, 2006, p 59−60.
(56) Bonin, J.; Costentin, C.; Louault, C.; Robert, M.; Routier, M.; Savéant, J.-M. *Proc. Natl. Acad. Sci. U.S.A.* **2010**, *107*, 3367.
(57) Costentin, C. *Chem. Rev.* **2008**, *108*, 2145.
(58) Newton, M. D.; Sutin, N. *Annu. Rev. Phys. Chem.* **1984**, *35*, 437.
(59) Winkler, J. R.; Gray, H. B. *Chem. Rev.* **1992**, *92*, 369.
(60) Gray, H. B.; Winkler, J. R. *Q. Rev. Biophys.* **2003**, *36*, 341.
(61) Turró, C.; Zaleski, J. M.; Karabatsos, Y. M.; Nocera, D. G. *J. Am. Chem. Soc.* **1996**, *118*, 6060.
(62) Markle, T. F. Ph.D. Dissertation, University of Washington, Seattle, WA, 2009.
(63) Inoue, Y.; Nakano, T.; Tanaka, H.; Kashiwa, N.; Fujita, T. *Chem. Lett.* **2001**, *30*, 1060.
(64) FluoFit Version 3.3. by PicoQuant GmbH. http://www.picoquant.com/
(65) Frisch, M. J.; Trucks, G. W.; Schlegel, H. B.; Scuseria, G. E.; Robb, M. A.; Cheeseman, J. R.; Scalmani, G.; Barone, V.; Mennucci, B.; Petersson, G. A.; Nakatsuji, H.; Caricato, M.; Li, X.; Hratchian, H. P.; Izmaylov, A. F.; Bloino, J.; Zheng, G.; Sonnenberg, J. L.; Hada, M.; Ehara, M.; Toyota, K.; Fukuda, R.; Hasegawa, J.; Ishida, M.; Nakajima, T.; Honda, Y.; Kitao, O.; Nakai, H.; Vreven, T.; Montgomery, J. A., Jr.; Peralta, J. E.; Ogliaro, F.; Bearpark, M.; Heyd, J. J.; Brothers, E.; Kudin, K. N.; Staroverov, V. N.; Kobayashi, R.; Normand, J.; Raghavachari, K.; Rendell, A.; Burant, J. C.; Iyengar, S. S.; Tomasi, J.; Cossi, M.; Rega, N.; Millam, J. M.; Klene, M.; Knox, J. E.; Cross, J. B.; Bakken, V.; Adamo, C.; Jaramillo, J.; Gomperts, R.; Stratmann, R. E.; Yazyev, O.; Austin, A. J.; Cammi, R.; Pomelli, C.; Ochterski, J. W.; Martin, R. L.; Morokuma, K.; Zakrzewski, V. G.; Voth, G. A.; Salvador, P.; Dannenberg, J. J.; Dapprich, S.; Daniels, A. D.; Farkas, Ö.; Foresman, J. B.; Ortiz, J. V.; Cioslowski, J.; Fox, D. J. *Gaussian 09*; Gaussian, Inc.: Wallingford, CT, 2009.
(66) Nelsen, S. F.; Blackstock, S. C.; Kim, Y. *J. Am. Chem. Soc.* **1987**, *109*, 677.
(67) Nelsen, S. F.; Weaver, M. N.; Luo, Y.; Pladziewicz, J. R.; Ausman, L. K.; Jentzsch, T. L.; O'Konek, J. J. *J. Phys. Chem. A* **2006**, *110*, 11665.
(68) This number represents an approximate average for the three phenol-base compounds as compared to the free 2,4,6-tri-*tert*-butylphenol. See Table S1 for the oxidation potentials of these four compounds.
(69) Linschitz and co-workers report that the CPET oxidation of *p*-methoxyphenol/pyridine by singlet tetracene shows a significant KIE, whereas the much faster reaction with triplet fullerene has no KIE.[12] In a later report, they report k_H/k_D ratios significantly greater than 1 for phenol/pyridine systems in benzonitrile, but no KIE when the added base is DMSO.[11] In general, KIE's greater than ∼6 are indicative of vibronic or vibrational nonadiabaticity, but a small KIE does not rule out a nonadiabatic CPET event because of confounding effects from proton donor−acceptor motion and contributions from excited vibronic states. Hammes-Schiffer, S.; Soudackov, A. V. *J. Phys. Chem. B* **2008**, *112*, 14108. Edwards, S. J.; Soudackov, A. V.; Hammes-Schiffer, S. *J. Phys. Chem. A* **2009**, *113*, 2117. Therefore, excited vibronic contributions are a plausible factor that can account for the small KIEs if the promoting modes in these systems are low-energy vibrations. As reported previously, a significant KIE is observed for all oxidations by aminium oxidants.[21,23]
(70) Fecenko, C. J.; Meyer, T. J.; Thorp, H. H. *J. Am. Chem. Soc.* **2006**, *128*, 11020.
(71) Huynh, M. H. V.; Meyer, T. J. *Chem. Rev.* **2007**, *107*, 5004.
(72) Eberson, L. *Adv. Phys. Org. Chem.* **1982**, *18*, 79.
(73) Farid, S.; Dinnocenzo, J. P.; Merkel, P. B.; Young, R. H.; Shukla, D.; Guirado, G. *J. Am. Chem. Soc.* **2011**, *133*, 11580.
(74) Farid, S.; Dinnocenzo, J. P.; Merkel, P. B.; Young, R. H.; Shukla, D. *J. Am. Chem. Soc.* **2011**, *133*, 4791.
(75) (a) Eberson, L. *Electron Transfer Reactions in Organic Chemistry*; Springer-Verlag: Berlin, Germany, 1987; Vol. 25, pp 27−35. (b) λ calculated from the self-exchange rate constant from Sorensen, S. P.; Bruning, W. H. *J. Am. Chem. Soc.* **1973**, *95*, 2445−2451 assuming an adiabatic reaction ($\lambda = 4\Delta G^{\ddagger}_{\text{self-exchange}}$).
(76) Amada, I.; Yamaji, M.; Sase, M.; Shizuka, H. *J. Chem. Soc. Faraday Trans.* **1995**, *91*, 2751.
(77) Anbazhagan, V.; Kathiravan, A.; Asha Jhonsi, M.; Renganathan, R. *Z. Phys. Chem.* **2007**, *221*, 929.
(78) Kojima, H.; Bard, A. J. *J. Am. Chem. Soc.* **1975**, *97*, 6317.
(79) Peover, M. E. *Oxidation and Reduction of Aromatic Hydrocarbon Molecules at Electrodes*; Wiley: New York, 1971, pp 259−281.
(80) Marcus, R. A. *J. Phys. Chem.* **1968**, *72*, 891.
(81) Marcus, R. A. *J. Phys. Chem. B* **2007**, *111*, 6643.
(82) Edwards, S. J.; Soudackov, A. V.; Hammes-Schiffer, S. *J. Phys. Chem. B* **2009**, *113*, 14545.
(83) Sutin, N. *Prog. Inorg. Chem.* **1984**, *30*, 441.
(84) Sutin's lower estimate derives from an analysis based on ET occurring at a distribution of distances. For uncharged reactants, Eberson estimates K_A to be 0.32, 0.86, and 1.84 M^{-1} for reaction distances of 5, 7, and 9 Å. Eberson, L. *Adv. Phys. Org. Chem.* **1982**, *18*, 79−185. Using these approximate values and the calculated separations of 9−13 Å (Table S5), an estimate of $K_A \sim 2$ M^{-1} is

made, leading to values of H_{ab} that are more nonadiabatic than the values presented above.
(85) Meyer, T. J.; Taube, H. *Electron transfer reactions*; Pergamon: New York, 1987; Vol. *1*, pp 331−384.
(86) Zhao, Y.; González-García, N.; Truhlar, D. G. *J. Phys. Chem. A* **2005**, *109*, 2012.
(87) Saveant, J.-M. *Energy. Environ. Sci.* **2012**, *5*, 7718.
(88) Costentin, C.; Robert, M.; Saveant, J.-M. *Phys. Chem. Chem. Phys.* **2010**, *12*, 11179.
(89) Sirjoosingh, A.; Hammes-Schiffer, S. *J. Phys. Chem. A* **2011**, *115*, 2367.
(90) Georgievskii, Y.; Stuchebrukhov, A. A. *J. Chem. Phys.* **2000**, *113*, 10438.
(91) Skone, J. H.; Soudackov, A. V.; Hammes-Schiffer, S. *J. Am. Chem. Soc.* **2006**, *128*, 16655.
(92) Moser, C. C.; Anderson, J. L. R.; Dutton, P. L. *Biochim. Biophys. Acta, Bioenerg.* **2010**, *1797*, 1573.
(93) The four-point calculation predicts a ∼0.4 eV smaller innersphere reorganization energy for **HOAr-Py** as compared to the unconjugated phenol bases. The difference of ∼0.2 eV in the total reorganization energy for the reaction with anthracene is obtained when taking into account the ∼0.2 eV calculated innersphere reorganization energy for the polyarenes via the additivity postulate and assuming λ_o = 0.5 eV for the outersphere reorganization energy of the phenols. The outersphere contributions for the polyarenes are calculated by eq S10. All of these contributions are combined using eqs S5 and S6 to calculate the total reorganization energy for the reaction.
(94) McCleskey, T. M.; Winkler, J. R.; Gray, H. B. *J. Am. Chem. Soc.* **1992**, *114*, 6935.
(95) Gould, I. R.; Farid, S. *Acc. Chem. Res.* **1996**, *29*, 522.